Kinetic studies of nitrate removal from aqueous solution using granular chitosan-Fe(III) complex

Qili Hu, Nan Chen, Chuanping Feng, Jing Zhang, Weiwu Hu and Long Lv

ABSTRACT

In the present study, a granular chitosan-Fe(III) complex was prepared as a feasible adsorbent for the removal of nitrate from an aqueous solution. There was no significant change in terms of nitrate removal efficiency over a wide pH range of 3–11. Nitrate adsorption on the chitosan-Fe(III) complex followed the Langmuir–Freundlich isotherm model. In order to more accurately reflect adsorption and desorption behaviors at the solid/solution interface, kinetic model I and kinetic model II were proposed to simulate the interfacial process in a batch system. Nitrate adsorption on the chitosan-Fe(III) complex followed the pseudo-first-order kinetic model and kinetic model I. The proposed half-time could provide useful information for optimizing process design. Adsorption and desorption rate constants obtained from kinetic model I and kinetic model II were beneficial to understanding the interfacial process and the extent of adsorption reaction. Kinetic model I and kinetic model II implied that nitrate uptake exponentially approaches a limiting value.

Key words | adsorption, chitosan-Fe(III) complex, kinetics, nitrate

Qili Hu
Nan Chen (corresponding author)
Chuanping Feng
Jing Zhang
Long Lv
School of Water Resources and Environment,
China University of Geosciences (Beijing),
Beijing 100083,
China
and
Key Laboratory of Groundwater Cycle and Environment Evolution (China University of Geosciences (Beijing)), Ministry of Education,
Beijing 100083,
China
E-mail: *chennan@cugb.edu.cn*

Weiwu Hu
The Journal Center,
China University of Geosciences (Beijing),
Beijing 100083,
China

INTRODUCTION

Adsorption is one of the most powerful techniques for wastewater purification including dyes, heavy metals and inorganic anions due to its convenience, ease of operation, simplicity of design and economic considerations (Bhatnagar & Sillanpää 2011). The adsorption of toxic molecules and ions on natural adsorbents might limit their spreading and reduce their harmful risks to ecosystem and human health (Marczewski 2010). Investigating a time dependent adsorption process was extremely necessary to predict kinetic parameters and understand the interfacial process at the solid/solution interface.

Nitrate contamination in surface water and groundwater has become a worldwide environmental problem, imposing a serious threat to drinking water supplies and promoting eutrophication (Ganesan *et al.* 2013). Nitrate was difficult to remove due to its high stability, high solubility and poor adsorption property (Loganathan *et al.* 2013). Hence, developing an easily reusable and environmentally friendly adsorbent was of utmost significance for the removal of nitrate.

The adsorption process could be described by four consecutive kinetic steps (Plazinski & Rudzinski 2010): (1) transport in bulk solution; (2) diffusion across liquid film surrounding adsorbent particles; (3) intraparticle diffusion; (4) adsorption and desorption on/from adsorbent surface considered as surface reaction, including chemical reaction or/and physical interaction. The overall rate of the adsorption process might be governed by any of these steps or by a combination of two steps (Haerifar & Azizian 2013).

There were various adsorption kinetic models employed to describe the kinetic data. The pseudo-first-order kinetic model (Lagergren 1898) and the pseudo-second-order kinetic model (Sobkowski & Czerwiński 1974) were the most popular and well-known adsorption kinetic models. Intraparticle diffusion model (Roginsky & Zeldovich 1934) could be used to judge whether intraparticle diffusion was the only rate-controlling step. Elovich model (Boyd *et al.* 1947) had general application to chemisorption kinetics. Their success undoubtedly reflected the ability to fit well with a wide variety of the experimental data. However, these kinetic models failed to reasonably evaluate adsorption and desorption behaviors at the solid/solution interface and provide the adsorption and desorption rate constants.

In this study, based on the pseudo-first-order and pseudo-second-order kinetic models, kinetic model I and

doi: 10.2166/wst.2015.596

kinetic model II were proposed for simulating the interfacial process at the solid/solution interface. The goodness of fit of various kinetic models was reasonably evaluated through correlation coefficient and chi-square analysis. Finally, the feasibility of kinetic model I and kinetic model II was investigated by analyzing the kinetics of nitrate adsorption on chitosan-Fe(III) complex.

MATERIALS AND METHODS

Materials

Chitosan (deacetylation degree = 80.0–95.0%) and sodium nitrate ($NaNO_3$) were purchased from Sinopharm Chemical Reagent Co., Ltd, Shanghai, China. Ethanol (CH_3CH_2OH) and Ammonia solution (25% w/w) were obtained from Beijing Chemical Works, Beijing, China. Ferric chloride ($FeCl_3$•$6H_2O$) was provided by Tianjin Fuchen Chemical Reagents Factory, Tianjin, China. A series of different concentrations of nitrate solution required were prepared with deionized water. All of the chemicals used in this study were of analytical grade without further purification.

Adsorbent synthesis

A given mass of chitosan powder was added into a beaker containing 300 mL 3.0% (w/w) $FeCl_3$ aqueous solution (pH = 1.78), and then continuously stirred at room temperature for 2.0 h. Chitosan could be thoroughly dissolved in this acid solution through protonation of $–NH_2$ functional group on the C-2 position of chitosan molecule (Rinaudo 2006). Subsequently, the resulting chitosan-Fe(III) solution was drop-wise added into an alkaline coagulating mixture (H_2O:NH_3•H_2O:CH_3CH_2OH 3:2:1, v/v) using a disposable syringe. After being stabilized for 1.0 h, the hydrogel beads that had formed were separated and sufficiently washed with deionized water, and then dried at 50 °C for 8.0 h in an oven (DL-101-2BS, Zhonghuan, China). The dried beads were immersed into deionized water at 40 °C for 4.0 h in a horizontal shaker (HZC-280, Peiying, China). After separation, washing and drying, the granular chitosan-Fe(III) complex obtained was kept in a sealed plastic bag at room temperature for further studies.

pH

50 mL of nitrate solution (50 mg L^{-1}) was poured into a series of conical flasks with 1.0 g of adsorbent, which was sealed and agitated at 120 rpm in a thermostatic shaker at room temperature for 2.0 h. The pH of the solution was adjusted using HCl or NaOH solution.

Kinetic experiments

100 mL of nitrate solution (20, 40, 50, 60, 80 and 100 mg L^{-1}) was poured into 250 mL conical flasks containing 2.0 g of adsorbent, which were agitated at 120 rpm and 20 °C in a thermostatic shaker. 1 mL sample solution was taken from conical flasks at certain time intervals (5, 10, 15, 20, 30, 45, 60, 75, 90 and 120 min) to analyze the residual nitrate concentration. Kinetic experiments were carried out in duplicate for each initial concentration to obtain better accuracy.

The amount of nitrate adsorbed per unit mass of adsorbent q_t (mg g^{-1}) was calculated using the following equation at time t (Ma *et al.* 2014):

$$q_t = \frac{(C_0 - C_t) \times V}{M} \quad (1)$$

where C_0 (mg L^{-1}) was the initial nitrate concentration; C_t (mg L^{-1}) was the nitrate concentration at time t; V (L) was the volume of nitrate solution; M (g) was the mass of adsorbent used.

Adsorption equilibrium

0.5 g of adsorbent was added to a series of conical flasks containing 50 mL of nitrate solution (30–180 mg L^{-1}). 1 mL sample was taken after 2.0 h to analyze the residual nitrate concentration under the same operating condition.

Analysis

Nitrate concentration was measured through a standard colorimetric method using a UV/vis spectrophotometer (DR 6000, HACH, USA). The pH value was determined by pH meter (SevenMulti S40, METTLER-TOLEDO, Switzerland).

THEORETICAL ANALYSIS

Understanding the reaction pathway and revealing rate-controlling mechanisms (diffusion, mass transfer, surface reaction, etc.) of the adsorption process were of prime importance for predicting the variation trend of nitrate uptake with time (Demarchi *et al.* 2013; Zhao *et al.* 2013). Thus,

establishing appropriate kinetic models was indispensable to adsorption studies. The differential equation of the pseudo-first-order kinetic model was expressed as (Tseng *et al.* 2014):

$$\frac{dq_t}{dt} = k_1(q_e - q_t) \tag{2}$$

where q_t (mg g^{-1}) and q_e (mg g^{-1}) were the amount of solute adsorbed per unit mass of adsorbent at time t and at equilibrium, respectively; k_1 (min^{-1}) was the pseudo-first-order rate constant; t (min) was the contact time.

After integrating Equation (2) at boundary conditions $t = 0$ to $t = t$ and $q_t = 0$ to $q_t = q_t$, the nonlinear and linear forms of the pseudo-first-order kinetic model were written as:

$$q_t = q_e[1 - \exp(-k_1 t)] \tag{3}$$

$$\ln(q_e - q_t) = \ln q_e - k_1 t \tag{4}$$

The differential equation of the pseudo-second-order kinetic model was expressed as (Igberase *et al.* 2014):

$$\frac{dq_t}{dt} = k_2(q_e - q_t)^2 \tag{5}$$

where k_2 (g mg^{-1} min^{-1}) was the pseudo-second-order rate constant.

The nonlinear and linear forms of the pseudo-second-order kinetic model after integration were written as:

$$q_t = q_e\left(1 - \frac{1}{1 + q_e k_2 t}\right) \tag{6}$$

$$\frac{t}{q_t} = \frac{1}{k_2 q_e^2} + \frac{1}{q_e}t \tag{7}$$

In many adsorption studies, Equations (4) and (7) have been frequently employed to estimate kinetic parameters by plotting $\ln(q_e - q_t)$ versus t and t/q_t versus t, respectively. Obviously, this drawing method failed to intuitively reflect the variation trend of nitrate uptake with time. Moreover, Ho (2006) reported that kinetic parameters obtained from four pseudo-second-order kinetic linear equations using the linear method were different, but they were the same when using the nonlinear method. This difference might be caused by each of these linear transformations changing the original error distribution (Kinniburgh 1986). A similar result was reported by Nouri *et al.* (2007) who pointed out that this linear transformation implicitly altered error structure and might also violate error variance and normality assumptions of standard least-square method. Consequently, in the present study, all of the kinetic parameters were calculated from nonlinear kinetic equations.

It was generally considered that adsorption was an interfacial phenomenon of solute spontaneously aggregating on adsorbent surface, which should include adsorption and desorption processes. The concentration of residual solute in aqueous solution remained constant when adsorption equilibrium occurred. It might as well be presumed that residual solute at equilibrium failed to participate in adsorption reaction. It was evident that the pseudo-first-order and pseudo-second-order kinetic models failed to give a desorption rate constant. Thus, it was difficult to know the extent of the adsorption reaction and how optimized experimental conditions were to promote equilibrium nitrate uptake. Consequently, it was extremely essential to modify them.

In order to logically establish kinetic models, initial content of solute in a batch system was converted to the amount of solute per unit mass of adsorbent, which was defined as follows:

$$Q = \frac{C_0 \times V}{M} \tag{8}$$

where Q (mg g^{-1}) was a constant only related to the initial content of solute and adsorbent mass.

In the present study, in order to remedy the defects of pseudo-first-order and pseudo-second-order kinetic models, kinetic model I and kinetic model II were first proposed to simulate the interfacial process in a batch system. The differential equation of kinetic model I was expressed as:

$$\frac{dq_t}{dt} = k_a(Q - q_t) - k_d q_t \tag{9}$$

where k_a (min^{-1}) and k_d (min^{-1}) were the adsorption and desorption rate constants of kinetic model I, respectively. The nonlinear form of kinetic model I after integration was given as:

$$q_t = \frac{k_a Q}{k_a + k_d}\{1 - \exp[-(k_a + k_d)t]\} \tag{10}$$

The differential equation of kinetic model II was expressed as:

$$\frac{dq_t}{dt} = k_a(Q - q_t)^2 - k_d q_t^2 \tag{11}$$

where k_a (g mg^{-1} min^{-1}) and k_d (g mg^{-1} min^{-1}) were the adsorption and desorption rate constants of kinetic model II, respectively. The nonlinear form of kinetic model II after integration was given as:

$$q_t = \frac{k_a Q}{k_a - k_d} - \frac{Q\sqrt{k_a k_d}}{k_a - k_d}\left[1 - \frac{2}{1 - \frac{\sqrt{k_a} + \sqrt{k_d}}{\sqrt{k_a} - \sqrt{k_d}}\exp\left(2Q\sqrt{k_a k_d}t\right)}\right] \tag{12}$$

Adsorption and desorption rate constants could be obtained from the nonlinear fitting curve of q_t versus t, which contribute to revealing reaction mechanisms of the interfacial process. It should be noted that when the adsorption process obeyed kinetic model I or kinetic model II, nitrate uptake exponentially approaches a limiting value for a given adsorption system due to both Equations (10) and (12) containing a time dependent exponent term. Therefore, adsorption occurred rapidly at the initial stage, followed by a sluggish step until equilibrium. This behavior was in agreement with the results of most adsorption studies. Moreover, the magnitude of adsorption and desorption rate constants could be utilized to judge the extent of adsorption reaction. The larger the ratio (k_a/k_d) was, the more thoroughly the adsorption reaction proceeded.

When adsorption reaction reached equilibrium, the changing rate of nitrate uptake with time was equaled to zero.

$$\frac{dq_t}{dt} = 0 \tag{13}$$

Substituting Equation (13) into Equations (9) and (11) led to

$$q_e = \frac{k_a Q}{k_a + k_d} \tag{14}$$

$$q_e = \frac{\sqrt{k_a} Q}{\sqrt{k_a} + \sqrt{k_d}} \tag{15}$$

The equilibrium nitrate uptake for each initial concentration could be calculated by Equations (14) and (15), respectively. It was not difficult to see that the equilibrium nitrate uptake was related to not only adsorption and desorption rate constants but also the initial content of solute and adsorbent dosage. Hence, optimizing these factors would promote equilibrium nitrate uptake.

By definition of

$$k_1 = k_a + k_d \tag{16}$$

and substituting Equations (14) and (16) into Equation (10) led to

$$q_t = q_e[1 - \exp(-k_1 t)] \tag{17}$$

For small values of $2Q\sqrt{k_a k_d}t$, we had the following mathematical approximation:

$$\exp(2Q\sqrt{k_a k_d}t) \approx 1 + 2Q\sqrt{k_a k_d}t \tag{18}$$

By definition of

$$k_2 = (\sqrt{k_a} + \sqrt{k_d})^2 \tag{19}$$

and substituting Equations (15), (18) and (19) into Equation (12) led to

$$q_t = q_e\left(1 - \frac{1}{1 + q_e k_2 t}\right) \tag{20}$$

It is worth mentioning that the pseudo-first-order rate constant was a combination of adsorption and desorption rate constants of kinetic model I, while Equation (19) reflected the complicated relationship between the pseudo-second-order rate constant and adsorption and desorption rate constants of kinetic model II. In general, the time required for the adsorption process to reach equilibrium was finite and, in some case, very short. Thus, the adsorption process followed kinetic model II or the pseudo-second-order kinetic model when the initial content of solute was not too high.

Moreover, in order to better understand the variation of solute concentration with time in a batch system, half-time was defined as the time required for the half amount of solute removal for kinetic model I and kinetic model II, which was expressed as:

$$q_t = \frac{Q}{2} \tag{21}$$

Substituting Equation (21) into Equations (10) and (12) led to

$$T_{\mathrm{I}} = \frac{1}{k_a + k_d}\ln\frac{2k_a}{k_a - k_d} \tag{22}$$

$$T_{II} = \frac{1}{2Q\sqrt{k_a k_d}} \ln \frac{\sqrt{k_a} + \sqrt{k_d}}{\sqrt{k_a} - \sqrt{k_d}} \quad (23)$$

Identifying the half-time of the adsorption process would contribute to knowing the variation trend of solute concentration in aqueous solution with time and providing useful information for optimizing process design.

RESULTS AND DISCUSSION

Repeatability evaluation

In this study, chitosan-Fe(III) complex had a narrow particle size ranging from 1.04 to 1.16 mm, suggesting that particle size of the adsorbent was relatively uniform. The repeatability among measured results was evaluated using standard deviation, which was given as follows (Frost *et al.* 2013):

$$\bar{C} = \frac{1}{k} \sum_{i=1}^{k} C_i \quad (24)$$

$$s = \sqrt{\frac{1}{k-1} \sum_{i=1}^{k} (C_i - \bar{C})} \quad (25)$$

where k was the number of the parallel samples; C_i (mg L^{-1}) and $\bar{C}$ (mg L^{-1}) were the one measured nitrate concentration and average nitrate concentration at equilibrium, respectively; s (mg L^{-1}) was the standard deviation.

The number of parallel samples in the present study was 16. The calculated s value was very small (0.065 mg L^{-1}), indicating that each measured result had a good repeatability.

Effect of pH

It was observed from Figure 1 that there was no significant change in terms of nitrate removal efficiencies (exceeding 72%) over a wide pH range of 3–11, and the final pH of solution was located between 5.4 and 6.0, indicating that nitrate adsorption was hardly affected by pH and that chitosan-Fe(III) complex had buffer capacity. Nitrate removal efficiency slightly reduced with increasing pH due to reduced protonation of the adsorbent.

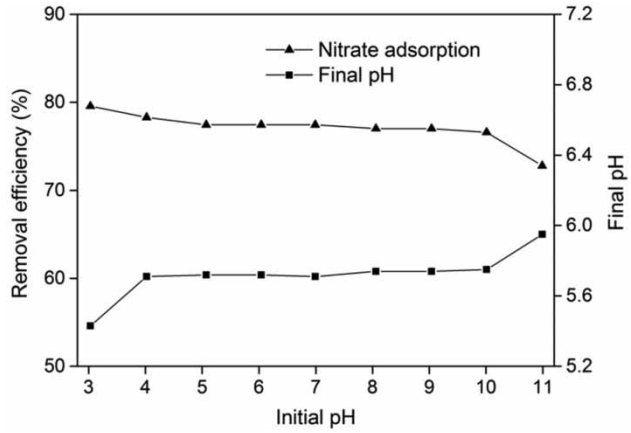

Figure 1 | Effect of pH on nitrate adsorption on chitosan-Fe(III) complex.

Kinetic studies

Pseudo-first-order and pseudo-second-order kinetic models

In addition to correlation coefficient (R^2), chi-square analysis (χ^2) was employed to reasonably examine the goodness of fit of various kinetic models, which was defined as (Mirmohseni *et al.* 2012):

$$\chi^2 = \sum \frac{(q_{exp} - q_{cal})^2}{q_{cal}} \quad (26)$$

where q_{exp} (mg g^{-1}) was the experimental nitrate uptake; q_{cal} (mg g^{-1}) was the calculated nitrate uptake. A smaller χ^2 value would reflect a better kinetic model.

The rapid interaction between solute and adsorbent was desirable and beneficial for practical applications. As shown in Figure 2, nitrate adsorption on chitosan-Fe(III) complex was rapid in the first 15 min, followed by a sluggish stage until equilibrium after around 60 min. In addition, it was observed that the variation trend of nitrate uptake with time was similar for different nitrate concentrations (data not shown). At the initial stage, available adsorption sites on an adsorbent surface and a concentration gradient between the bulk solution and adsorbent surface were high (Islama & Patel 2010). With the increase in the adsorption time, the adsorption rate gradually decreased because available adsorption sites on adsorbent surface and residual nitrate in aqueous solution reduced. The high initial adsorption rate and the short equilibrium time implied that the surfaces of chitosan-Fe(III) complex had a high density of active sites for nitrate adsorption and

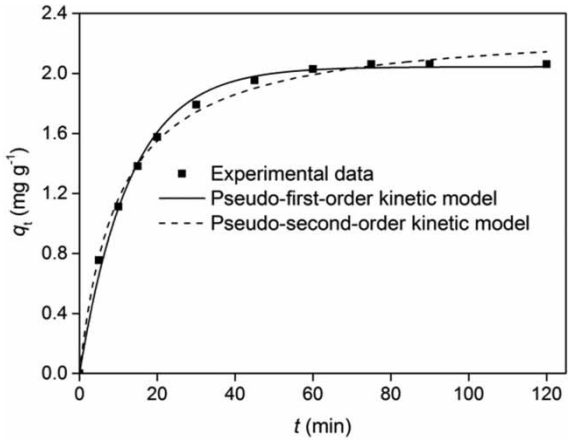

Figure 2 | Kinetic studies of nitrate removal with an initial concentration of 50 mg L^{-1} (as N).

adsorption mainly took places on the surfaces (Li *et al.* 2005). Accordingly, chitosan-Fe(III) complex had the ability to remove more nitrate ions in a much shorter time.

It could be clearly seen from Tables 1 and 2 that compared with the pseudo-second-order kinetic model, the equilibrium nitrate uptake obtained from the pseudo-first-order kinetic model was almost equal to the experimental nitrate uptake and that the pseudo-first-order kinetic model had a higher correlation coefficient and lower chi-square value for each initial concentration. Consequently, nitrate adsorption on chitosan-Fe(III) complex obeyed the pseudo-first-order kinetic model. It should be noted that the equilibrium nitrate uptake obtained from the pseudo-first-order kinetic model was lower than the experimental nitrate uptake, while the equilibrium nitrate uptake obtained from the pseudo-second-order kinetic model was higher than the experimental nitrate uptake. This behavior might be attributed to the different mathematical forms of Equations (3) and (6). Similar results were reported by Raji & Pakizeh (2014).

Table 1 | Kinetic parameters obtained from the pseudo-first-order kinetic model

C_0 (mg L^{-1})	q_{exp} (mg g^{-1})	q_{cal} (mg g^{-1})	k_1 (min^{-1})	R^2	χ^2
20	0.94	0.93	0.0879	0.9995	4.96×10^{-5}
40	1.68	1.68	0.0737	0.9992	2.73×10^{-4}
60	2.40	2.38	0.0690	0.9980	1.38×10^{-3}
80	2.89	2.88	0.0654	0.9975	2.54×10^{-3}
100	3.33	3.31	0.0594	0.9964	4.71×10^{-3}

Table 2 | Kinetic parameters obtained from the pseudo-second-order kinetic model

C_0 (mg L^{-1})	q_{exp} (mg g^{-1})	q_{cal} (mg g^{-1})	k_2 (g mg^{-1} min^{-1})	R^2	χ^2
20	0.94	1.05	0.1124	0.9912	9.09×10^{-4}
40	1.68	1.93	0.0484	0.9926	2.56×10^{-3}
60	2.40	2.75	0.0311	0.9950	3.48×10^{-3}
80	2.89	3.34	0.0238	0.9955	4.62×10^{-3}
100	3.33	3.88	0.0178	0.9959	5.58×10^{-3}

The effect of initial nitrate concentration on k_1 and k_2 was depicted in Figure 3. It was obvious that the values of the pseudo-first-order and pseudo-second-order rate constants decreased with the increase in initial nitrate concentration. Herein, k_1 and k_2 were the observed rate constants of the overall adsorption reaction rather than the intrinsic rate constants. As a matter of fact, a larger rate constant demonstrated that a shorter time required for reaching specific removal efficiency (Ghodbane & Hamdaoui 2008). It could be concluded that nitrate ions was removed rapidly in an adsorption system with a lower initial concentration. Additionally, no linear relationship was observed between rate constants and initial nitrate concentration, suggesting that adsorption mechanism of nitrate adsorption on chitosan-Fe(III) complex was not unique and that the rate-determining step was different at various initial concentrations.

Kinetic model I and kinetic model II

The fitting results of kinetic model I and kinetic model II were illustrated in Figure 4. Compared with the experimental nitrate uptake, there were −0.89 and 1.66% relative error for the equilibrium nitrate uptake obtained from kinetic

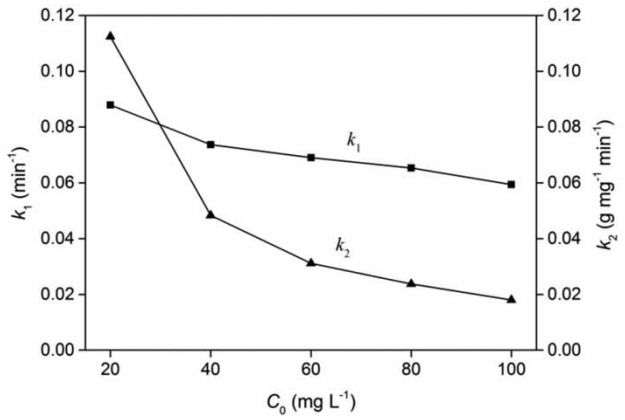

Figure 3 | The plot of k_1 and k_2 versus C_0 for nitrate adsorption on chitosan-Fe(III) complex.

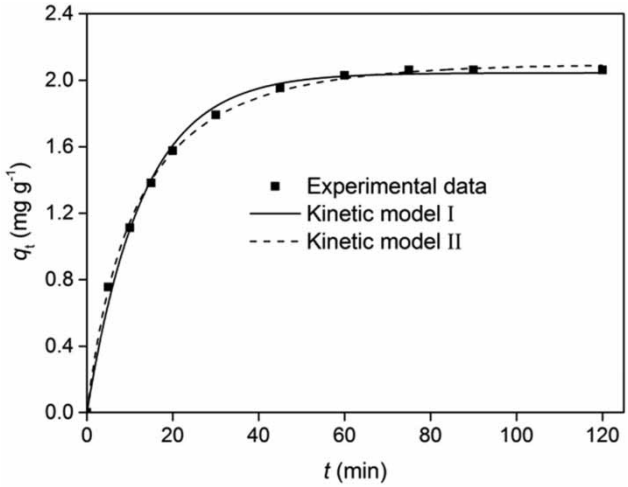

Figure 4 | Kinetic studies of nitrate removal with an initial concentration of 50 mg L^{-1} (as N).

model I and kinetic model II, respectively. Nitrate uptake increased rapidly with time, reaching 2.06 mg g^{-1} at equilibrium.

As shown in Tables 3 and 4, kinetic model I and kinetic model II having high correlation coefficient and low chi-square value for each initial concentration agreed well to the experimental results in the range of allowable error. Besides, the equilibrium nitrate uptake obtained from kinetic model I was almost equal to the experimental nitrate uptake. These results indicated that nitrate adsorption on chitosan-Fe(III) complex obeyed kinetic model I. Moreover, it was not difficult to find that half-time increased significantly with the increase in initial nitrate concentration. Therefore, it was essential to adjust nitrate concentration to shorten half-time in a batch system.

The influence of initial nitrate concentration on adsorption and desorption rate constants of kinetic model I and kinetic model II was illustrated in Figure 5. It was evident that adsorption rate constant decreased while desorption rate constant increased with the increase in initial nitrate concentration. There was no doubt that the number of available adsorption sites on adsorbent surface was limited for a certain amount of adsorbent. As a result, available adsorption sites were not enough to hold continuously increasing nitrate ions, resulting in the increase in residual nitrate ions in aqueous solution. Moreover, the adsorption trend increased at lower concentration and the desorption trend increased at higher concentration, which were consistent with the theoretical analysis.

On the other hand, it was found that the fitting results of kinetic model I and the pseudo-first-order kinetic model were identical in terms of nitrate uptake, correlation coefficient and chi-square value for each initial concentration. This result was due to the fact that Equation (10) was converted to Equation (3) by means of variable substitution, and thereby their mathematical expression was identical. Furthermore, the observed rate constant of the pseudo-first-order kinetic model was a combination of adsorption and desorption rate constants of kinetic model I for each initial concentration,

Table 3 | Kinetic parameters obtained from kinetic model I

C_0 (mg L^{-1})	q_{exp} (mg g^{-1})	q_{cal} (mg g^{-1})	k_a (min^{-1})	k_d (min^{-1})	T (min)	R^2	χ^2
20	0.94	0.93	7.89×10^{-2}	9.01×10^{-3}	9.27	0.9995	4.96×10^{-5}
40	1.68	1.68	6.05×10^{-2}	1.32×10^{-2}	12.74	0.9992	2.73×10^{-4}
60	2.40	2.38	5.16×10^{-2}	1.74×10^{-2}	15.99	0.9980	1.38×10^{-3}
80	2.89	2.88	4.48×10^{-2}	2.06×10^{-2}	20.04	0.9975	2.54×10^{-3}
100	3.33	3.31	3.76×10^{-2}	2.18×10^{-2}	26.35	0.9964	4.71×10^{-3}

Table 4 | Kinetic parameters obtained from kinetic model II

C_0 (mg L^{-1})	q_{exp} (mg g^{-1})	q_{cal} (mg g^{-1})	k_a (g mg^{-1} min^{-1})	k_d (g mg^{-1} min^{-1})	T (min)	R^2	χ^2
20	0.94	0.99	11.84×10^{-2}	2.43×10^{-4}	8.16	0.9912	9.13×10^{-4}
40	1.68	1.74	4.03×10^{-2}	1.27×10^{-3}	12.21	0.9965	1.24×10^{-3}
60	2.40	2.44	2.02×10^{-2}	1.89×10^{-3}	16.05	0.9992	5.58×10^{-4}
80	2.89	2.93	1.24×10^{-2}	2.36×10^{-3}	20.55	0.9994	6.12×10^{-4}
100	3.33	3.35	0.79×10^{-2}	2.51×10^{-3}	27.21	0.9984	2.15×10^{-3}

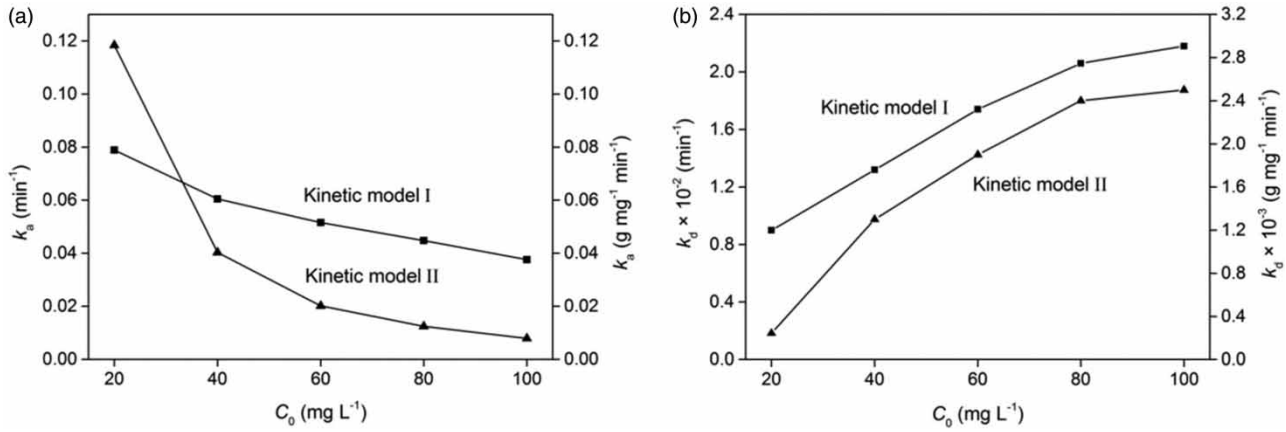

Figure 5 | The plot of adsorption (a) and desorption (b) rate constants versus initial nitrate concentration for kinetic model I and kinetic model II.

which was in agreement with the theoretical analysis. Kinetic model I provided adsorption and desorption rate constants, which contributed to understanding the adsorption process at the solid/solution interface. Thus, kinetic model I was superior to the pseudo-first-order kinetic model. Compared with the pseudo-second-order kinetic model, kinetic model II not only had higher correlation coefficient and lower chi-square value for each initial concentration, but also provided the fitting nitrate uptake closer to the experimental nitrate uptake. There were few deviations between rate constants for kinetic model II and the pseudo-second-order kinetic model using Equation (19), implying that this mathematical approximation in theoretical analysis was reasonable.

Adsorption isotherm

In this study, equilibrium data were analyzed by the Langmuir (Nouri *et al.* 2007), Freundlich (Ma *et al.* 2014) and Langmuir–Freundlich (Demarchi *et al.* 2013) isotherm models. The nonlinear forms of these models were expressed as:

$$q_e = \frac{q_m K_L C_e}{1 + K_L C_e} \tag{27}$$

$$q_e = K_F C_e^{1/n} \tag{28}$$

$$q_e = \frac{q_m K_{F-L} C_e^m}{1 + K_{F-L} C_e^m} \tag{29}$$

where q_e (mg g^{-1}) was the amount of nitrate adsorbed per unit mass of adsorbent at equilibrium, C_e (mg L^{-1}) was the equilibrium nitrate concentration, K_L (L mg^{-1}) was the Langmuir constant, q_m (mg g^{-1}) was the fitting maximum adsorption capacity, K_F ((mg g^{-1}) (L mg^{-1})$^{1/n}$) was the Freundlich constant, n was an empirical parameter, K_{F-L} (L mg^{-1}) was the Langmuir–Freundlich constant, and m was the heterogeneity factor.

Figure 6 intuitively described how close the fitted curve was to the experimental data points for the three isotherm models. As shown in Table 5, compared with Langmuir isotherm, Freundlich isotherm provided the smaller χ^2 and higher R^2 values, indicating that the Freundlich isotherm fitted with equilibrium data was superior to the Langmuir isotherm and that the Langmuir isotherm could not accurately predict the maximum adsorption capacity. It was not difficult to see that the results provided by Langmuir–Freundlich isotherm agreed well with experimental data. Therefore, the maximum adsorption capacity was 7.46 mg g^{-1}.

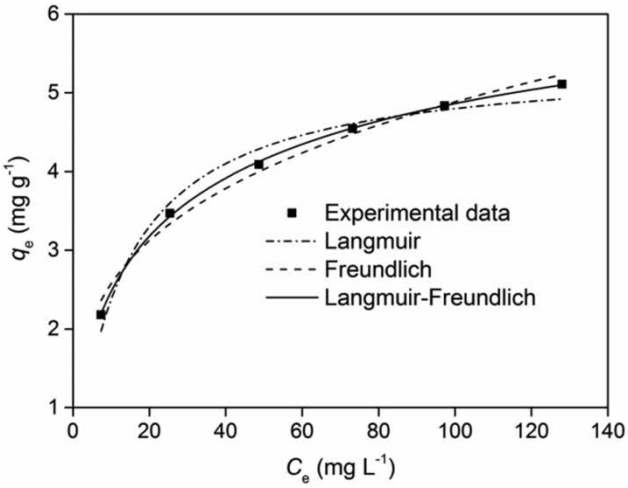

Figure 6 | Adsorption isotherm for nitrate adsorption on chitosan-Fe(III) complex.

Table 5 | Error analysis and parameters of the Langmuir, Freundlich, and Langmuir–Freundlich models

Langmuir		Freundlich		Langmuir–Freundlich	
q_m (mg g^{-1})	5.41	K_F ((mg g^{-1}) (L mg^{-1})$^{1/n}$)	1.36	q_m (mg g^{-1})	7.46
K_L (L mg^{-1})	7.82×10^{-2}	n	3.60	K_{L-F} (L mg^{-1})	0.13
				m	1.74
χ^2	3.51×10^{-2}	χ^2	1.97×10^{-2}	χ^2	9.70×10^{-4}
R^2	0.970	R^2	0.983	R^2	0.999

CONCLUSIONS

Granular chitosan-Fe(III) complex successfully removed nitrate from aqueous solution. The adsorption of nitrate on chitosan-Fe(III) complex was hardly affected by pH and maximum adsorption capacity provided by Langmuir–Freundlich isotherm reached 7.46 mg g^{-1} (as N). Nitrate adsorption on chitosan-Fe(III) complex obeyed the pseudo-first-order kinetic model and kinetic model I. The application of various kinetic models for analyzing the experimental data showed that: (i) the pseudo-first-order and pseudo-second-order rate constants decreased with the increase in initial nitrate concentration; (ii) adsorption and desorption rate constants provided by kinetic model I and kinetic model II contributed to understanding the interfacial process in a batch system and judging the extent of adsorption reaction; and (iii) kinetic model I and kinetic model II implied that nitrate uptake exponentially approached a limiting value.

ACKNOWLEDGEMENTS

The authors acknowledge financial support from the National Natural Science Foundation of China (NSFC) (No. 21407129, No. 51578519), the Beijing National Science Foundation (No. 8144053), and the Fundamental Research Funds for the Central Universities (No. 2652015123).

REFERENCES

Bhatnagar, A. & Sillanpää, M. 2011 A review of emerging adsorbents for nitrate removal from water. *Chemical Engineering Journal* **168** (2), 493–504.

Boyd, G. E., Adamson, A. W. & Myers Jr, L. S. 1947 The exchange adsorption of ions from aqueous solutions by organic zeolites. II. Kinetics. *Journal of the American Chemical Society* **69** (11), 2836–2848.

Demarchi, C. A., Campos, M. & Rodrigues, C. A. 2013 Adsorption of textile dye reactive red 120 by the chitosan–Fe(III)-crosslinked: batch and fixed-bed studies. *Journal of Environmental Chemical Engineering* **1** (4), 1350–1358.

Frost, J., Keller, K., Lowe, J., Skeete, T., Walton, S., Castille, J. & Pal, N. 2013 A note on interval estimation of the standard deviation of a gamma population with applications to statistical quality control. *Applied Mathematical Modelling* **37** (4), 2580–2587.

Ganesan, P., Kamaraj, R. & Vasudevan, S. 2013 Application of isotherm, kinetic and thermodynamic models for the adsorption of nitrate ions on graphene from aqueous solution. *Journal of the Taiwan Institute of Chemical Engineers* **44** (5), 808–814.

Ghodbane, I. & Hamdaoui, O. 2008 Removal of mercury(II) from aqueous media using eucalyptus bark: kinetic and equilibrium studies. *Journal of Hazardous Materials* **160** (2–3), 301–309.

Haerifar, M. & Azizian, S. 2013 An exponential kinetic model for adsorption at solid/solution interface. *Chemical Engineering Journal* **215–216**, 65–71.

Ho, Y. S. 2006 Second-order kinetic model for the sorption of cadmium onto tree fern: a comparison of linear and non-linear methods. *Water Research* **40** (1), 119–125.

Igberase, E., Osifo, P. & Ofomaja, A. 2014 The adsorption of copper (II) ions by polyaniline graft chitosan beads from aqueous solution: equilibrium, kinetic and desorption studies. *Journal of Environmental Chemical Engineering* **2** (1), 362–369.

Islama, M. & Patel, R. 2010 Synthesis and physicochemical characterization of Zn/Al chloride layered double hydroxide and evaluation of its nitrate removal efficiency. *Desalination* **256** (1–3), 120–128.

Kinniburgh, D. G. 1986 General purpose adsorption isotherms. *Environmental Science and Technology* **20** (9), 895–904.

Lagergren, S. 1898 About the theory of so-called adsorption of soluble substances. *Kungliga Svenska Vetenskapsakademiens Handlingar* **24**, 1–39.

Li, N., Bai, R. & Liu, C. 2005 Enhanced and selective adsorption of mercury ions on chitosan beads grafted with polyacrylamide via surface-initiated atom transfer radical polymerization. *Langmuir* **21** (25), 11780–11787.

Loganathan, P., Vigneswaran, S. & Kandasamy, J. 2013 Enhanced removal of nitrate from water using surface modification of adsorbents – a review. *Journal of Environmental Management* **131**, 363–374.

Ma, J., Shen, Y., Shen, C., Wen, Y. & Liu, W. 2014 Al-doping chitosan–Fe(III) hydrogel for the removal of fluoride from aqueous solutions. *Chemical Engineering Journal* **248**, 98–106.

Marczewski, A. W. 2010 Analysis of kinetic Langmuir model. Part I: integrated kinetic Langmuir equation (IKL): a new complete analytical solution of the Langmuir rate equation. *Langmuir* **26** (19), 15229–15238.

Mirmohseni, A., Seyed Dorraji, M. S., Figoli, A. & Tasselli, F. 2012 Chitosan hollow fibers as effective biosorbent toward dye: preparation and modeling. *Bioresource Technology* **121**, 212–220.

Nouri, L., Ghodbane, I., Hamdaoui, O. & Chiha, M. 2007 Batch sorption dynamics and equilibrium for the removal of cadmium ions from aqueous phase using wheat bran. *Journal of Hazardous Materials* **149** (1), 115–125.

Plazinski, W. & Rudzinski, W. 2010 A novel two-resistance model for description of the adsorption kinetics onto porous particles. *Langmuir* **26** (2), 802–808.

Raji, F. & Pakizeh, M. 2014 Kinetic and thermodynamic studies of Hg(II) adsorption onto MCM-41 modified by $ZnCl_2$. *Applied Surface Science* **301**, 568–575.

Rinaudo, M. 2006 Chitin and chitosan: properties and applications. *Progress in Polymer Science* **31** (7), 603–632.

Roginsky, S. Z. & Zeldovich, Y. B. 1934 The catalytic oxidation of carbon monoxide on manganese dioxide. *Acta Physical Chemistry USSR* **1**, 554–594.

Sobkowski, J. & Czerwiński, A. 1974 Kinetics of carbon dioxide adsorption on a platinum electrode. *Journal of Electroanalytical Chemistry* **55** (3), 391–397.

Tseng, R. L., Wu, P. H., Wu, F. C. & Juang, R. S. 2014 A convenient method to determine kinetic parameters of adsorption processes by nonlinear regression of pseudo-nth-order equation. *Chemical Engineering Journal* **237**, 153–161.

Zhao, Y., Yang, S., Ding, D., Chen, J., Yang, Y., Lei, Z., Feng, C. & Zhang, Z. 2013 Effective adsorption of Cr (VI) from aqueous solution using natural Akadama clay. *Journal of Colloid and Interface Science* **395**, 198–204.

First received 3 July 2015; accepted in revised form 10 November 2015. Available online 24 November 2015